Hydrol. Earth Syst. Sci. Discuss., 10, 625–674, 2013
www.hydrol-earth-syst-sci-discuss.net/10/625/2013/
doi:10.5194/hessd-10-625-2013
© Author(s) 2013. CC Attribution 3.0 License.

Hydrology and
Earth System
Sciences
Discussions

This discussion paper is/has been under review for the journal Hydrology and Earth System Sciences (HESS). Please refer to the corresponding final paper in HESS if available.

Pertinent spatio-temporal scale of observation to understand sediment yield control factors in the Andean Region: the case of the Santa River (Peru)

S. B. Morera[1,2], T. Condom[3], P. Vauchel[4], J.-L. Guyot[5], C. Galvez[6], and A. Crave[7]

[1]Geosciences Environnement Toulouse, 14 avenue Edouard-Belin, Toulouse, France
[2]Universidad Agraria La Molina, Av. Universidad s/n, La Molina, Lima 12, Peru
[3]Laboratoire d'étude des Transferts en Hydrologie et Environnement – LTHE – UMR 5564, Université Joseph Fourier – Grenoble 1, IRD–Great Ice, CNRS, G-INP, Grenoble, France
[4]Laboratoire des Mécanismes de Transferts en Géologie – UMR 5563 – CNRS-UPS-IRD, Toulouse, France
[5]Institut de Recherche pour le Développement, Lima, Peru
[6]Special project CHAVIMOCHIC, Trujillo, Peru
[7]Geosciences Rennes, Centre National of Research Scientific, Rennes, France

Received: 16 December 2012 – Accepted: 25 December 2012 – Published: 15 January 2013

Correspondence to: S. B. Morera (sergiobaymorera@gmail.com)

Published by Copernicus Publications on behalf of the European Geosciences Union.

Title Page
Abstract | Introduction
Conclusions | References
Tables | Figures
|◀ | ▶|
◀ | ▶
Back | Close
Full Screen / Esc
Printer-friendly Version
Interactive Discussion

Abstract

Hydro-sedimentology development is a great challenge in Peru due to limited data as well as sparse and confidential information. Consequently, little is known at present about the relationship between the El Niño Southern Oscillation (ENSO), precipitation, runoff, land use and the sediment transport dynamics. The aim of this paper is to bridge this gap in order to quantify and understand the signal of magnitude and frequency of the sediment fluxes from the central western Andes; also, to identify the main erosion control factor and its relevance.

The Tablachaca River (3132 km^2) and the Santa River (6815 km^2), two mountainous Andean catchments that are geographically close to each other, both showed similar statistical daily rainfall and discharge variability but high contrast in sediment yield (SY). In order to investigate which factors are of importance, the continuous water discharge and hourly suspended sediment concentrations (SSC) of the Santa River were studied. Firstly, the specific sediment yield (SSY) at the continental Andes range scale for the Pacific side is one of the highest amounts (2204 t km^2 yr^{-1}). Secondly, no relationship between the water discharge (Q) and El Niño/La Niñ a events is found over a 54 yr time period. However, the Santa Basin is highly sensitive during mega Niños (1982–1983 and 1997–1998). Lastly, dispersed micro-mining and mining activity in specific lithologies are identified as the major factors that control the high SSY. These remarks make the Peruvian coast key areas for future research on Andean sediment rates.

1 Introduction

Understanding erosion control factors is a great challenge in order to improve the modelling of continental and mountain range dynamics or climate change and human impacts on the environment. Numerous studies address this fundamental question by looking generally at a specific scale and at some specific potential factors such as: climate (e.g. Farnsworth and Milliman, 2003; Kirchner et al., 2001; Milliman and Syvitski, 1992; Pépin et al., 2010; Riebe et al., 2001; Carretier et al., 2012), tectonics (e.g. Ahnert, 1970; Pinet and Souriau, 1988; Lavé and Avouac, 2001), rainfall (e.g. Bookhagen et al., 2005; Safran et al., 2005; Fang Fang et al., 2012; Lin et al., 2008), topography (e.g. Verstraeten and Poesen, 2001; Safran et al., 2005), land use and vegetation (e.g. Cerdan et al., 2010; Zhang et al., 2008), lithology (e.g. Aalto et al., 2006; Molina et al., 2008), seismicity (Dadson et al., 2003; Pépin et al., 2010) and human activities (e.g. Zhang and Wen, 2004; Wohl, 2006; Houben et al., 2009; Syvitski and Kettner, 2011; Walling, 2006; Slaymaker, 2010). The erosion rate includes many processes, from the rock alteration process to mass transport processes. Most of the studies dealing with erosive processes focus on a few of these processes at a local scale range ($< 1\,\text{km}^2$) due to the difficulty of in-situ or experimental monitoring (Cerdan et al., 2010) in order to follow all implied chemical and physical forcing. For scales larger than $1\,\text{km}^2$, most studies try to point out the specific empirical statistical relationship between the SSY at the outlet of the watersheds and "factors", which are usually not the chemical or physical quantities involved in the chemical kinetics or the action of the mechanical forces. Most of these factors are only boundary conditions of the chemical and physical forcing of the erosion process. For example, the concept of climate encompasses many chemical and physical variables such as rainfall, which in turn encompasses the statistical distribution of several chemical and physical variables such as water volume, intensity, kinetic energy or chemical components. All of these quantities only indirectly control the alteration and the sediment detachment and transport processes. Therefore, a large combination of factor strengths could lead to a similar erosive efficiency and, inversely, the variation of one factor can hardly explain the erosion rates alone. Furthermore, the dominance of one erosive process in terms of the SSY amplitude, among others, is relative to the scale, and the impact of the factors on the SSY is strongly dependent on how the spatial heterogeneity of the factor strength can be integrated into the upscaling process. Due to all of the above reasons, there is currently no clear relationship and the hierarchy has been set between the monitored so-called erosion factors and the SSY (Vente et al., 2011) on a large-scale range. Most of the analyses of the worldwide data present a large statistical dispersion (Syvitski et al., 2003; Vanmaercke et al., 2011) and cannot be used to design an easy-use universal empirical or physical model.

One of the best ways to analyse the factors which control the SSY is studying the topographic system with a few potential factors that have large gradients, while considering all of the other factors to be constant. Mountain ranges are good candidates for this approach because they are the places with the largest erosion rates and large climate changes, slope gradients and seismicity processes. Among mountain ranges worldwide, the Andes range is a particular and interesting geological object because it crosses all terrestrial climate configurations from north to south, and presents sharp climatic gradients from east to west, passing from a tropical climate to the world's driest desert in its central part, respectively. Montgomery et al. (2001) show that, at the Andes scale, the topography characteristics match the mean annual precipitation and the theoretical erosion index intensity (product of the local slope with the upstream rainfall amount). These authors suggest that this correlation indicates that climate is a first-order factor for the topographic evolution of the Andes. This conclusion implicitly assumes that: (i) the dynamic of the topography of the Andes is in dynamic equilibrium with the rainfall variability, (ii) rainfall is not mainly controlled by the topography, and (iii) erosion is linearly related to the upstream rainfall amount and the slope value. Three hypotheses are debated in the discussion regarding feedback between climate, tectonic and erosion forcing (Lamb and Davis, 2003; Molnar and England, 1992; Raymo and Ruddiman, 1992).

Another approach used to analyse factor control on the SSY is to analyse modern SSY databases. Due to the limited amount of available public SSY data in the Andean watersheds, only a few studies undertake a synthetic analysis of the relationship between the erosion factors and the SSY (Aalto et al., 2006; Armijos et al., 2013; Laraque et al., 2009; Molina et al., 2007, 2008; Pépin et al., 2010; Restrepo et al., 2006; Guyot, 1993). In the northern part of the Andes, the mean annual runoff explains most of the SSY variations in the Magdalena River watershed and sub-watersheds (Restrepo et al., 2006). Note that Restrepo et al. (2006) only prospect hydrologic, morphometric and climatic factors and cannot prospect vegetation, soil properties and the effect of land uses because of the lack of information on these parameters. Conversely, Aalto et al. (2006) do not show any relationship between runoff and the SSY with a database on 47 Bolivian watersheds. On the other hand, the lithology and the slopes show the best correlations with the SSY in the Bolivian front size of the Andes. Note that the former study is mainly focused on geomorphic, hydrologic and lithologic parameters without any information about vegetation or land-use parameters. Pépin et al. (2010) carried out a complete study of the SSY in 66 Chilean watersheds with similar sizes along the Andes from the extreme north of Chile to Southern Patagonia, covering a wide range of climate, slopes and vegetation. This former study points out that the SSY shows a linear relationship with the slope and runoff, respectively, both above and below the threshold values related to the vegetation cover. Lithology and seismicity are also prospected but do not give reliable results due to the non-exhaustiveness of these data in Chile. At the hillslope scale ($< 1\,\text{km}^2$), Molina et al. (2007, 2008) show that the SSY is well correlated to the cover, soil types and road networks using a database on 37 small sub-watersheds of the Paute River (Ecuador). Despite the particular climatic configuration of the Andes, these studies cannot give a clear view of the relative dominance of the erosion control factors.

A spatial overview of the available SSY data from the central and northern Andes (Fig. 1) – for an overview of the SSY in the Southern Andes, the reader can refer to Pépin et al. (2010) – shows that there is almost no published data on the SSY of the central Andes along the Pacific coast of Peru. In fact, reliable data on the SSY from the Peruvian pacific side of the Andes are scarce and part of them are monitored by private companies. However, this area has a large climatic gradient, from an Equatorial climate in the northern part to a desert climate in the southern part. Furthermore, climate variability in the central Andes is closely linked to the ENSO (Aceituno, 1988; Garreaud and Aceituno, 2001; Marengo and Tomasella, 1998; Rao et al., 2002; Soden, 2000). For example, in the north west of the Andean Cordillera, both high discharge and high

CC BY

sediment load are found during the La Niña phase; in contrast, these are low during the El Niño phase (Restrepo and Kjerfve, 2000). However in the case of Peru (Lavado et al., 2012) report that, there is no clear evidence of increased rainfall and runoff on the northern coast during El Niño, except for some extreme events (1982/1983 and 1997/1998) but further studies may clarify their results. So, currently little is known about the influence of ENSO on regional-scale climate variability. Consequently, the relationship between ENSO, precipitation, runoff, and the sediment transport dynamics of the central Andes are poorly understood.

In this paper, a new daily SSY dataset on the central Andes in Peru is analysed thanks to a collaboration between the Chavimochic (http://www.chavimochic.gob.pe/) and Hybam (http://www.orehybam.org/) projects. Reliable SY data has been collected since 1999 by the Peruvian irrigation Chavimochic project. It follows the monitoring of sediment in the lower part of the Santa River watershed at three hydrosedimentology stations. The study area is located in the central western part of the Andes. The Santa River catchment is characterized by strong altitudinal gradients, with a high contrast variability from the sea to the highest point in the central Andes (6768 m a.s.l.; Nevado Huascaran). The seasonal and low vegetation cover, the poor consolidate lithology, as well as the weather all change significantly over relatively short distances and the rainfall gradient from east/west runs from 0 to 1,150 mm yr^{-1} (1998–2010). In addition, there is intense human activity such as the small and large mining of coal, metal and aggregate distributed from the coast to the highland (Morera, 2010).

The aim of this study is to better understand the magnitude and frequency of the SSY from the central western Andes to the Pacific coast, with a special focus on: (i) the influence of the ENSO on the SSY; and (ii) the main erosion control factor and its relevance. At the very least, this analysis also emphasizes that in order to compare the SSY datasets in the Andes, the criteria need to be better defined in order to define the so-called control factors and the scale at which they have to be analysed.

2 Study area and settings configuration

2.1 Main geographic description of Santa and Tablachaca watersheds

The Santa River is the largest river that empties into the Pacific Ocean off Peru, with a total length of 316 km and a drainage area of 12 000 km^2. It is situated in the northwest of Peru, between 7.9–10.3° S and 78.6–77.2° E. This study focuses on two sub-watersheds that are geographically close to each other (Fig. 2): the Santa station (507 m a.s.l.), covering the middle and upper Santa basin (6815 km^2), and the Tablachaca station (524 m a.s.l.), which monitors the whole Tablachaca sub-watershed (3132 km^2), are both sub-watersheds that are part of the Santa River Basin which is monitored at the Condorcerro station (479 m a.s.l., 9969 km^2).

The Santa sub-watershed drains from southeast to northwest and is defined by the Cordillera Blanca at the east side and the cordillera Negra at the west side (Fig. 2). Furthermore, the Cordillera Blanca is located in the western branch of the Andes in Peru; it is also the highest and most extensive expanse of tropical glaciers in the world (Zapata et al., 2008). Second, it is the only example of an active, large-magnitude extension with a pronounced footwall topography (McNulty and Farber, 2002). Another of its important characteristics is that it represents approximately 35 % (600 km^2) of the total area of the Peruvian glaciers and ~ 10 % of the total watershed; also, it contains the Huascaran peak at 6768 m a.s.l., which is the highest point in the central Andes (Georges, 2004). Finally, the Santa sub-watershed has a rugged topography with slopes that exceed 100 % in the higher parts of the range, and it contains more than 15 peaks above 6 km (Schwartz, 1988). In contrast, the Tablachaca sub-watershed extends from northeast to southwest of the high mountain ranges which reach ~ 5000 to 479 m a.s.l. In the first place, the natural setting of the Tablachaca sub-watershed creates highly vulnerable watersheds with deeper and smaller rivers than the Santa sub-watershed; consequently, the rivers discharge disproportionately large quantities of sediment along the Tablachaca River.

The characterization of the main river slope in the Santa sub-watershed is divided by a knickpoint at the Canyon "Del Pato" level, and it is gradually expanding upstream to the river origin, forming plate areas (68 %); also, in most cases, there tends to be low slopes (0–17°), as will be shown in part 2.

2.2 Lithology

The regional geology includes pyrite, schists, phyllite, pyrite-bearing, and quartzite material intruded by a central granodiorite-tonalite batholith that is all overlain by clastic sediments deposited during the glacial retreat (Wilson et al., 1967). Although many of the granite/granodiorite boulders possess weathering posts, the quartzite and felsic volcanic boulders are commonly devoid of weathering features, and most of the quartzite boulders still possess glacial polish and striae (Schwartz, 1988). On the other hand, the seasonal and low vegetation cover with a very heterogeneous lithology (Fig. 3), have few stable soils overall and conglomerates that are predominantly clasts. Those are grouped into metapelites from the Jurassic Chicama Formation, volcanic rocks from the Tertiary Calipuy Formation, rhyolite probably from the Tertiary Calipuy Formation (rather than the poorly consolidated Tertiary Yungay ignimbrites), and granite from the Cordillera Blanca batholith. In terms of altitude, the lower 900 m are dominated by clasts from the Tertiary Calipuy Formation; nevertheless, granite clasts first appear above 900 m (Giovanni et al., 2010). Ultimately, the Chimu formation is located in a series of coal basins (Table 1), from the Palaeozoic to the Cenozoic age variable and normally related with the different orogenic events which strongly affected this region (Carrascal-Miranda and Suárez-Ruiz, 2004). However, the most important distributions came from Mesozoic-Chimu coal in the Santa Basin (Petersen, 2010).

2.3 Mining activity

Significant human effort went into mining and mineral production in ancient Peru; this human activity dominated the landscape of the inter-Andean valleys on a temporal scale ranging from years to centuries (Harden, 2006; Petersen, 2010). Ever since the Spanish conquered the Andes, this zone has been known for its deposits of gold, silver, coal and other valuable metals (United-Nations, 1990). Thus, the element coal was used during pre-Inca times for metallurgy, and the first large-scale industrial application occurred around 1816 for steam generation at copper mines (Agramonte and Diaz, 1983). An example of the vast reserve of minerals within the Santa watershed is found in the largest known Cu-Zn skarn ore deposit, “Antamina” (e.g. Fig. 4), and it incorporates a mineral reserve of 561 Mt (Love et al., 2004). Overall, the Santa Basin presents significant environmental problems, most of which are due to abandoned mine tailing stocks and the related problem of mine closure, poorly maintained tailing ponds, competition for scarce water resources and highly polluting smelters (McMahon et al., 1999). As a consequence, the water quality in the Upper Santa River watershed is threatened by historical and present-day mining and increasing near-stream disposal of domestic, industrial and mining waste as well as livestock grazing (Young and Lipton, 2006; BCRP, 2009).

For centuries, large-scale and artisanal mining have posed a widely dispersed environmental liability risk. Still, there is little information on the spatiotemporal variations of the current large-scale and artisanal mining activities because the mining regulations are not well enforced and the mines are typically located in remote areas (Tarras-Wahlberg and Lane, 2003). On the other hand, the Tablachaca and Santa watersheds have steepened slopes due to agriculture, construction and mining practices. Consequently, differences in the soil properties are associated with differences in the land cover and land use (Harden, 2006). Finally, and most convincingly, due to their configuration, the mountains are very vulnerable to erosion due to mining waste which represents environmental liabilities that could cause a collapse, producing large amounts of sediment and landslides that could form natural dams.

2.4 Slope degree

A complex relationship between sediment flux and slope angle was found as a result of a detailed analysis of the trajectory of the soil particles during raindrop impact (DePloey and Savat, 1968); in addition, a formula in which the flux rates should be proportional to the sine of the slope angle for soil creep based on the cyclic wetting and drying was derived (Kirkby, 1967). For example, at lower slopes ($< 15^\circ$) McKean et al. (1993) and Small et al. (1999) estimated flux rates using cosmogenic radionuclides and found a linear relationship between the gradient and sediment flux on gentle slopes. Nonetheless, as the slopes approach 31–41°, the sediment flux is a highly nonlinear function of the slope (Roering et al., 1999).

2.5 Hydro-climatology context

The annual mean precipitation shows high variability with a range between 10 and 1150 mm from west to east in the study area. It is characterized by two distinct climates with a high contrast variability gradient from the sea to the Andean Cordillera (e.g. Smith, 1979). In the first climate zone, the arid coast is situated in the lowlands to the west of the Andes. This desert area is generated by the southerly cold wind coming from the Pacific Ocean surface and it forces subsidence in order to maintain a thermal balance, triggering drying within this region, which maintains an inversion layer at about 1000 m a.s.l. Moreover, the mean unseasonal annual precipitation less than 10 mm is common in stations along the coast and over the pre-Andean Central Depression (at about 1000 m a.s.l.). Finally, most of this amount is due to drizzle from the coastal stratus and very unusual rainfall episodes associated with the passage of a cold front (Garreaud and Fuenzalida, 2007; Garreaud and Rutllant, 1996; Vargas et al., 2006). In the second climate zone, there are semiarid mountain chains in the middle and upper basin. Precipitation in this region is dominated by the southward expansion of the upper-tropospheric easterlies during the austral summer, associated with the intensification of the South American summer monsoon (Garreaud, 2009). Nonetheless, the precipitation values decrease when the northern tropical Atlantic Ocean is warmer than usual (Lavado et al., 2012). The daily precipitation variation is more frequent and stronger during the afternoon and evening during the rainy season (Garreaud, 1999). On average, 90 % of the annual total precipitation falls from October to April, with a peak in precipitation in February and March; consequently, stream flows dramatically increase 10 to 30 fold during the wet season. The rest of the year (May–September) is rather dry, with less than 50–100 mm total precipitation (Vuille et al., 2008). In the end, surface runoff in the upper basin of the Santa River originates from rainfall and glacier snowmelt on the Cordillera Blanca (Mark and Seltzer, 2003). During the dry season, groundwater accounts for 18 to 74 % of the water entering some basins, with the difference coming from glacier meltwater (Baraer et al., 2009; Condom et al., 2012).

3 Data and methodology

3.1 Geomorphologic parameters

Nowadays, various datasets with geo-information are available, making it possible to derive catchment parameters from the Shuttle Radar Topography Mission (SRTM) 3 arcsec (~ 90 × 90 m) DEM distributed by the USGS data centre (http://seamless.usgs.gov/). The accuracy of the general dataset was calculated as a 6.2 height error absolute by Rodríguez et al. (2006); however, Racoviteanu et al. (2007) estimate differences of 25 m at higher elevations and steeper slopes (glaciers). The basic configuration of the geomorphology, such as the mean slope, catchment surface areas, river networks, and height differences within each catchment were calculated using GIS tools. Finally, the analysis of the erosion rates was carried out by quantifying the slopes on the sides of the basin in order to find traces or relationship between the slopes and lithological formations, following Bryan (2004).

3.2 Lithological map

First, lithological information was collected from geological studies carried out by the National Development Institute (INADE) and journal publications. Second, Fig. 3 was made considering the lithological nature of the bedrock and formation age, both of which were simplified into eight different types (Table 1) based on the works of Giovanni et al. (2010) and Carrascal-Miranda and Suárez-Ruiz (2004). A detailed structural lithological field mapping was performed at the 1 : 100 000 scale. We would like to point out that for this part of the research, punctual monitoring was carried out in the main sub-watersheds of the Santa Basin during a two year period in the wet and dry seasons. Therefore, we compare the sub-watersheds that have a higher significant sediment load and the lithology map. Last, the statistical analysis and GIS processing was performed with an evaluation of the slope distribution for each lithology.

3.3 Land use

The land use is processed from Lansat-7 ETM images using high resolution data (30 × 30 m); and eventually, this information is downloaded from the Earth Explorer page, which is available for the USGS (http://edcsns17.cr.usgs.gov/NewEarthExplorer/).

This part of the research is divided into two phases: we evaluate the main land cover areas, using GPS points that are well distributed throughout the watershed such as forests, crops, slide areas, rocks, mining, towns, glaciers, water bodies and areas of dark soil due to exposed coal. The second phase, carried out with ERDAS software, involved the supervised classification of land cover following Göttlicher et al. (2009), based on the GPS points already taken in the catchment, as well as the use of Google Earth as a visual aid to view the points that could not be physically reached (glaciers).

First and foremost, we downloaded three image mosaics to encompass the entire study area for the year 2006; then, the analysis is derived by the classification of bands 2, 3 and 4 of the Landsat-7 ETM image (Adams et al., 1995). Another important

cc BY

characteristic is that these mosaics date from June to July 2006 because this is a period of relative stability for the ecological system; for example, the vegetation cover could change month by month from 100 to 50 % area cover. Furthermore, we can better analyse the Landsat image due to fewer clouds at the research zone. The mosaic images are georeferenced, normalized and characterized in six dominant types of land cover: rock, glacier, woodland, urban, mine and bare soil. Finally, the distribution area within each slope degree is calculated in percentage using GIS (e.g. Tao et al., 2012; Ward et al., 2009).

3.4 New available hydro-sedimentology data

Accurate estimates of the SYs depend on effective monitoring strategies (Duvert et al., 2011). Since 1999, the Peruvian irrigation Chavimochic project has been following the monitoring of the instantaneous *Q* from instantaneous limnigraph readings and calibration curve, and hourly samples of SSC in the lower part of the Santa River watershed at the Condorcerro station, two years after it started to do so at the Santa and Tablacha stations. Thus, the first step is to collect the widely dispersed information and then process it. As a result, an unpublished database is available with two SSC samples per day (Fig. 5), and instantaneous *Q* limnigraph readings (Fig. 6). Nevertheless, the physical and anthropogenic controls on the SY analysis are complex; therefore, this study uses an extensive database to increase the understanding of the relationships between the SY and the environmental variables at the catchment scale in the Andes.

Sample numbers of the SSC and *Q* available at the gauging stations are evaluated considering an average resolution of two samples per day (06:00 a.m. and 06:00 p.m. LT) for each station. After that, the monthly percentage of the available data is calculated for each month and by season. This means that the month of January (31 days) must have 62 SSC readings; then, this month is considered to be a month with 100 % data. The evidence suggests that there are more problems with the Santa station in terms of data gaps compared to the Tablachaca and Condorcerro stations due to the lack of water level records and the low frequency of sediment sampling. Ultimately, gaps in the information on the SSC per month are fully completed using the rating curve equation (Fig. 8), due to a high coefficient correlation ($R > 0.9$, $p < 0.0001$).

Figure 5 exhibits the annual cycle in which we can observe a high seasonal contrast, but in both cases, a permanent flux is shown during the dry season due to glacier melt and ground water contribution. Apart from that, we observed that the daily Q series at the Tablachaca station showed higher variability than the Santa station because of the lower reception area and greater longitudinal river slope.

3.5 Rainfall information

The climatic parameters are calculated from the Yungay (2537 m a.s.l.; −9.14992° S; −77.75103° W) and Cabana (3300 m a.s.l.; −8.3531° S −78.00201° W) rainfall stations. Daily precipitation records were taken by the national Peruvian institution of meteorology and hydrology (SENAMHI). This climatic information was processed to calculate the probability density function (PDF, Fig. 7).

4 Result

4.1 Analysis of time-series of outflow discharges

The mean daily Q ($\mathrm{m^{-3}\,s^{-1}}$) from the Santa, Tablachaca and Condorcerro stations are estimated from instantaneous Q. The statistics for the Tablachaca and Santa stations at a 95 % confidence interval (C.I.) showed an average daily Q of 27.6 and 113 $\mathrm{m^{-3}\,s^{-1}}$ and standard deviations (S.D.) of 28.7 and 91.8, respectively. The high variability in the intense and prolonged rainfall in the region is mostly related to El Niño events. An analysis between the mean daily Q measurement time series (Fig. 6), and weak, moderate and strong Niño and Niña events is carried out to identify the relationship between discharges (extreme events at daily peak flow in $\mathrm{m^3\,s^{-1}}$ and annual volume in $\mathrm{km^3\,yr^{-1}}$) and the El Niño/La Niñ a events compiled in Table 2.

The ENSO phenomena is an inter-annual climate oscillation between anomalous warm phases (El Niño) and enhanced cold phases (La Niña) (Philander, 1983). A long time series of Q from 1957 to 2010 (Fig. 6) was used to estimate and characterize the daily and annual hydrological condition above the ENSO for the Condorcerro catchment. In addition, the terms in Table 2 are based on the Multivariate ENSO Index (MEI) and are classified by NASA. Events are defined as five consecutive months at or above the +0.5 °C Sea Surface temperature (SST) anomaly for warm (El Niño) events and at or below the −0.5 SST anomaly for cold (La Niña) events. The threshold is further broken down into weak (with a 0.5 to 0.9 SST anomaly), moderate (1.0 to 1.4) and strong (≥ 1.5) events. Detailed information is provided at http://ggweather.com/enso/oni.htm.

In Fig. 6, a strong daily peak and annual discharge were observed for the 1982–1983 and 1997–1998 periods, when the El Niño was strong; nevertheless, discharges in normal years produces almost the same annual volume (i.e. 1983–1984, 1993–1994). Looking at other years, the same volume is produced by a weak Niña (1984–1985) and a moderate Niño (1994–1995), whereas a strong Niña event (1988–1989) doubles the annual flow that that observed for a strong Niño event (1991–1992). Given these results, there is no direct relationship between ENSO events and either the daily Q or the annual volume for the Santa catchment at the Condorcerro monitoring station.

4.2 Rainfall, Q and SSC statistics

Frequency distribution analyses are useful to describe the distribution of Q (Turcotte and Greene, 1993), floods (Malamuda and Turcotte, 2006), hazardous events (Korup and Clague, 2009) and sediment fluxes (Hovius et al., 2000; Lague et al., 2005) in natural systems. A frequency distribution analysis provides information on whether the probability of a magnitude event follows a specific trend, which expresses how natural systems control the statistics of variables such as rainfall intensity, river Q or the SSC. The frequency distributions are more interesting as they follow an analytic probability density function model because the probabilities of the apparition and weight of a specific magnitude event can be derived mathematically. Therefore, frequency distributions are powerful criteria to compare hydrological responses. In this study, we focus on the daily rainfall, Q and concentration of both the Tablachaca and Santa watersheds without carrying out detailed analyses. A simple comparison of the magnitude–frequency distributions gives information on whether or not the variables of both basins follow the same statistical trends. Note that a proper PDF comparison requires normalization by the statistical average of the variable in each sampling population (Fig. 7).

The PDF of the daily rainfall and discharge values have similar trends for both the Santa and Tablachaca watersheds (Fig. 7a and b), despite a different annual specific mean runoff, i.e. 15 and 9 mm, respectively. This indicates that both watersheds have a similar hydrological response. They differ only by the amplitude of the Qs, which are relative to the drainage area and rainfall rate of each watershed. On the contrary, the PDF of the SSC for both watersheds differs significantly for concentrations larger than the respective averages. The PDF of the SSC for the Santa and Tablachaca watersheds follow a monotonic decreasing power law and non-monotonic trends, respectively. This indicates different erosion and sediment transport responses to identical hydrological inputs. Figure 8 shows the whole sediment data available from 2002 to 2010 for the Tablachaca and Santa stations with a coefficient $R > 0.9$ for $N = 11\,467$ taken every 12 h ($p < 0.0001$). The rating curves between the specific Qs and the suspended sediment concentration ($[\mathrm{SSC}] = a\,Q^b$) highlight this difference between both watersheds (Fig. 8). The power law exponents of the rating curves are similar (i.e. $b = 1.8 \pm 0.1$) if we take into account the uncertainties on the exponent value determination. Again, this means that the response to hydrological inputs is identical in both watersheds and does not vary much over the entire hydrological cycle. The coefficient a marks the main difference in terms of the erosive output and suggests that the Santa and Tablachaca watersheds have contrasted sediment availability. For an equivalent specific discharge, the SSC of the Tablachaca River is on average nine times larger than the SSC of the Santa River. Note that the Tablachaca's rating curve shows a rather stable high SSC value ($\sim 350\,\mathrm{mg\,L^{-1}}$) for specific discharges below a threshold value of $3 \times 10^{-3}\,\mathrm{m^3\,s^{-1}\,km^{-2}}$. During the low water season, when most of the watershed is under very dry climate conditions, the SSC of the Tablachaca River varies between 150 mg L^{-1} and 3 g L^{-1} and in the field, it is possible to see highly contrasted water colour at stream confluences (Fig. 4). This indicates a powerful source of sediment localized in the channel that does not depend on the *Q*. Also note that for the Tablachaca River and for large *Q*s during the rainy season, the SSC shows a larger fluctuation around the rating curve, indicating that hydrological control on sediment production is more fluctuant than in the Santa watershed.

4.3 Specific Sediment Yield (SSY)

The mean annual estimated SSY for the Tablachaca watershed is 2204 ± 337 t km^2 yr^{-1}, which is three times greater than the SSY for the Santa watershed 779 ± 162 t km^2 yr^{-1} (Table 3) despite the fact that the abundant water resources of the Santa River are four times greater than those of the Tablachaca watershed. Although the Tablachaca and Santa watersheds are geographically close to each other, the standard deviations showed two different SSY ratios. It should be noted that this period does not include the mega Niños, during which the highest discharges could be expected.

To summarize, the SSY in the outlet of the Tablachaca catchment presents one of the highest erosion rates in the entire Andes even though these values do not include bedload fluxes, which still need to be estimated.

4.4 Slope, lithology and land use analysis

Besides *Q*, there could be many different erosion factors. For example, slope, soil/lithological properties, vegetation and land uses are commonly cited as being related to erosion rates (e.g. Bryan, 2004). The study areas present a variety of slopes from hillfronts to piedmont and arid surfaces over different lithologies. The Tablachaca basin shows a larger surface with slope values between 7 and 25° than the Santa basin (Fig. 9). However, the Santa basin has more surfaces with slope values smaller than 7°

and larger than 25°. Such relative spatial slope distribution does not provide arguments to explain the contrast in erosion rates between the two basins.

Particular differences between arable land and other land uses will also affect soil erosion and hence SY (Montgomery, 2007; Vanacker, 2005). We found dispersed open pit micro-mining and mining activity in the Tablachaca and Santa catchments: 4 and 8 % of the total watershed surface respectively; remains of glaciers: 1 % and 7 % respectively; woodland areas: 39 and 32 % respectively; scraggly and seasonal cover vegetation (bare soil) 48 and 46 % respectively, as well as an urban cover of 9 and 7 % respectively. As a result, the main dominant land uses in the Tablachaca and Santa watersheds are bare soil and woodland (Fig. 10). This analysis, based on six types of land cover, does not show any major contrast in the spatial distribution of land uses between the Santa and Tablachaca catchments, but during the monitoring, it was observed that there is a high density of underground micro-mining located in a specific watershed composed of a specific lithology (e.g. the Chimu and Chicama formations). The evidence suggests that a typical remote sensing analyst could not quantify the underground mines.

The Tablachaca and Santa catchments show differences in terms of the spatial distribution of the lithologies (Table 1 and Figs. 3 and 11). The Chimu, Calapuy and Chicama formation areas are 5, 2.1 and 1.5 times higher respectively in the Tablachaca watershed than in the Santa watershed. Conversely, the areas comprising the Granodiorite and fluvio glacier formations are 5 and 14 times higher respectively in the Santa watershed than in the Tablachaca watershed. Besides the fluvio-glacier formation, which is one of the least cohesive lithologies observed on both watersheds, it is rather difficult to properly quantify the relative cohesiveness of each formation. Therefore, the results for the relative surface of each lithology cannot be specifically balanced with a simple coefficient of cohesiveness specifically for the watersheds where mining activities are well developed.

Figures 10 and 11 show a cross-analysis with the slope distribution for each type of land use and lithology. If we focus this analysis on the two main land use types, i.e.

cc BY

woodland and bare soil, the slope distribution is different only for bare soils in the Santa watershed with a higher proportion of steepest slopes. For each lithology formation, the slope distribution in the Tablachaca watershed does not show steeper slopes than those of the Santa watershed. Actually, if it is assumed that the erosion rates increase with steeper slopes, weighting areas of land use and lithology formations with slope distribution do not provide any arguments to explain the difference in the erosion rates between the two watersheds.

5 Discussion

Based on the daily monitoring of the Q and SSC at the confluence of the Tablachaca and Santa Rivers, new insights into the control factors of hydrology, sediment fluxes and erosion rate in the Andes can be discussed.

5.1 ENSO control on the hydrology and sediment flux of the Santa River

The ENSO is often associated with consistent climate anomalies throughout South America (e.g. Garreaud, 2009; Vuille et al., 2008; Ronchail and Gallaire, 2006). In this study, high Q events occur randomly and do not show any evidence of correlation with large Niño events. This was also observed in the hydrology of the basin outlet (Lavado et al., 2012) and the climatology at the Nevado Huascaran in the upstream part of the Santa watershed by Henderson et al. (1999) and Georges (2009). Note that various quantitative criteria are used to scale Niño events (Singh et al., 2011) and they may not be pertinent to estimate a correlation with hydrology. Furthermore, a study of this type needs large time series to cover a significant statistic amount of various Niño events and this present study may not cover a sufficiently large enough time series. But at a time scale of 54 yr of monitoring, the relationship between hydrology and Niño events is not straightforward in the area of the Santa Basin. Nevertheless, positive correlations are expected in the presence of mega Niño events (1982–1983 and 1997–1998) because of the landslides and huge sediment loads.

5.2 SSC vs. runoff rating curve

The correlation between the SSC and runoff has been examined to define the rating parameters that are usually used to compare Q control on the SSC for different watersheds (Ferguson, 1986; Walling, 1977). The rating curves for the Tablachaca and Santa Rivers are well defined and the sensitivity of the SSC to Q, denoted by exponent b of the rating curve, is the same and homogeneous in both watershed areas. This result supports the hypothesis that the sediment transport processes are similar at the Santa and Tablachaca watershed scale. However, the availability of sediment for transport through the river networks, denoted by coefficient a, is nine times larger for the Tablachaca watershed. Note that below the runoff threshold, there is evidence of a sediment source that induces a high concentration in the Tablachaca River during the dry season independently of the Q variation. This may be induced by informal gold exploration in the Tablachaca river bed which takes place during the dry season. These informal mining activities stop during the rainy season because it is difficult to access the river bed and therefore these activities cannot explain the constant difference in terms of sediment availability throughout the entire range of runoff values. At least three conceptual watershed erosion configurations can explain the constant gap between the rating curves over the entire runoff range. Configuration one: the Tablachaca area has a larger homogeneous erodibility than the Santa area. Configuration two: both channel networks have an unlimited alluvial sediment stock and the erodibility of the alluvial sediment is larger in the Tablachaca's channel network.

Configuration three: both watersheds have heterogeneous spatial erodibility with a large contrast in the values and the spatial runoff distribution is stable on both watersheds irrespective of the global daily runoff intensity. Both watersheds have various slopes, land uses and lithology spatial distribution and it would be unlikely that all of the characteristics of these different areas result in a homogeneous erodibility. Therefore, configuration one seems to be unrealistic. To validate configuration two, we need to more fully explore, in the field, the mechanical properties of the sediment sources in the Tablachaca and Santa valley bottoms. Soft material coming from landslide products, mine tailing and river bed material exploitation can be seen quite often at different places in both channel networks (Fig. 4). But extensive monitoring at many points of the river is necessary to properly quantify the respective suspended sediment production from each different type of sediment stock. In any case, there is no straightforward explanation as to why the alluvial sediments of the Tablachaca River are nine times more erodible than those of the Santa River. Indeed, in order to follow the variability of the sediment sources, there needs to be more detailed monitoring. In order to validate configuration three, we need to explore the daily rainfall distribution at a spatial resolution equivalent to the smallest domain size that is likely to control the sediment production of each watershed: for example, specific land-use and/or lithologic areas. The resolution of the land-use and lithology maps is of the order of 10 km^2. Rain-gauge station networks are too sparse over the study area to produce precipitation maps at this resolution. Satellite TRMM data provide reliable rainfall data for large-scale analysis (Bookhagen and Strecker, 2008). However, the local-scale analysis of the spatiotemporal rainfall distribution using TRMM data requires specific calibrations with the local rainfall datasets from the gauging stations (Andermann et al., 2011). Currently, there is no reliable rainfall dataset with high spatial resolution for the Santa and Tablachaca catchments and we cannot check the relevance of configuration three.

5.3 Sediment Yield (SY) control factors

Contrasted SYs provide interesting data that can be used to reveal the control factors of erodibility. Many previous works try to point out the empirical relationships between the potential factors, for example: climate (Riebe et al., 2001; Kirchner et al., 2001; Farnsworth and Milliman, 2002), uplift rate (Bonnet and Crave, 2003), slope (Lague et al., 2000), vegetation (Molina et al., 2008), land use (Molina et al., 2012), mining (Betancourt et al., 2005) or lithology (Aalto et al., 2006), with the SY in the river. Most of the previous analyses show correlation and regression with large dispersion that could be linked to a non-negligible uncertainty (Vanmaercke et al., 2011; Syvitski and Milliman, 2007). Standard inter-comparisons of the SSY between watersheds indicate several sources of uncertainties. Among the most important are the errors induced by the nature of most of the current factors mentioned in previous studies which do not correspond to the “direct” physical factors involved in the sediment alteration and transport processes. This means that these factors are neither dragging nor lifting forces that apply a shear stress on the sediment particles. Most of these factors are only the boundary conditions of the mechanical or chemical processes of the landscape erosion. Each of the boundary factors can change more or less the amplitude of the “direct” factors and several combinations of boundary factor intensity can lead to the same response from the erosive processes. Another source of uncertainties is the implicit assumption that the intensity of many control factors is linearly related to their area of extension such as land uses, lithology or sediment stocks. This assumption is poorly verified for factors that are more related to volume units such as landslides, sediment stock in the alluvial plain or also related to anthropic activity such as mining in a specific lithology domain.

This study is a nice illustration of how difficult it is to clearly define the control factors of the SSY. The Tablachaca and Santa watersheds do not show any contrasts in the major boundary control factor that could explain the relatively high SY at the outlet of the Tablachaca. For example, Restrepo (2000) identified Colombian watersheds that have high soil erosion because of the high precipitation rates (∼ 7200 mm). In this research, the lack of argument may be induced by our methodology which includes several sources of error (see above), and/or a discharge and concentration dataset that does not describe the spatial SSY gradients with a suitable resolution. Previous studies have already mentioned the difficulty to get inside information about the erosion boundary control factor by looking at the sediment flux at the outlet of a watershed (Vanmaercke et al., 2011). Actually, more precise field investigations are necessary to better understand the SSY contrast between the watersheds, i.e. better understand the relationship between the boundary and direct erosion factors. Two field campaigns were conducted with water sampling along the channel networks of the Tablachaca and Santa Rivers to track the sediment sources during the dry season. These data show a high heterogeneous spatial distribution of the concentrations with values of two different orders of magnitude between the Tablachaca's tributaries. The mineralogy composition of the highest SSC was carried out in the X-ray laboratories of the Geological, Mining and Metallurgical Institute (INGEMMET). The results from the samples showed that the concentration is made up of orthoquartzites, siltstones, sandstones, shales and coal beds and that it primarily matches the mineralogy of the Chimu formation (Carrascal-Miranda and Suárez-Ruiz, 2004). The lithology of the Chimu formation corresponds respectively to 11 and 1 % of the Tablachaca and Santa areas. This observation appears to be coherent with the SSY contrast between both watersheds. Furthermore, the highest incidence of mining is observed for the Chimu lithology in the Tablachaca watershed. Based on these observations, these authors assume that lithology and mining are the main control factors that explain the SSY contrast. However, this assumption should also explain the difference in sediment availability observed over the entire discharge range, i.e. during the rainy season for which there is no field campaign data, due to the rugged and unsafe configuration of the study area with very strong slopes (that can exceed 100 %), fast flow variation and mining protection rules.

5.4 Specific Sediment Yield (SSY) vs. runoff in the Andeans

Sharp unexplained SSY spatial contrasts could induce misinterpretation in the analysis of erosion control factors at global scale. We can illustrate this point with a compilation of the SSY vs. runoff data on the central and north part of the Andes from previous studies (Fig. 12, Table 3). Following this dataset there is no evidence of runoff control on SSY. There is no clear trend between both variables and the highest specific yield match the most arid region of the dataset. But actually there is no doubt that runoff is one of the main control factors of SSY. First, because Q is intrinsically related to the water velocity in the river, ie. to the main variable which cause mechanical shear stress and transport process. Second, because rating curves between sediment concentration and Q are statistically significant despite the dispersion of the data.

This study shows that the runoff dependency of the SSY analysis at a global scale should be carefully managed to filter other significant control factors. The average annual runoff is not the relevant variable to set the empirical relationship between the runoff and SSY. Both the statistical Q distribution and the rating curve parameters control the annual average of the runoff. The intercept and potential thresholds of the rating curve mark the dependency of other SSY factors and could be specific to each watershed. Any empirical analysis of SSY dependency should clearly take into account the distinction between these parameters.

6 Conclusions

Thanks to the long time series of high frequency data (2 measurements per day) from 1999 to 2010, this study provides an important contribution to quantify the SSY in two Andean catchments: the Tablachaca and Santa catchments, which are connected at the Condorcerro station. For the Santa and Tablachaca watersheds, the specific liquid discharge and the precipitation rates are similar but a high difference exists between the mean annual SSY values which are equal to 779 and 2204 $\mathrm{t\,km^2\,yr^{-1}}$ respectively. The sediment production of the Tablachaca watershed is one of the highest amount in the whole Andes range. To explain the differences in the sediment production between the two sub-watersheds, the main factors are analysed.

This analysis identified dispersed micro-mining and mining activity, which is developed in a specific lithology formation, as the major causative factors explaining the rate of high erosion. However, it is not only the limitations in the data resolution but also the large complexity and extreme contrast in the study area that makes it difficult to explain whether one of them control the high SSY at the catchment scale. Indeed, these findings confirm earlier studies conducted around the world indicating that the relationship between the SSY and controlling factors is often complex.

During the 1957–2010 period, a high variability of Q is shown and is consistent with the precipitation variability; nevertheless, the role of the ENSO is not clear. In other words no clear relationship between the ElNiño/La Niña events with the sediment production at the scale of 54 yr was found; however, the Santa Basin is very sensitive during mega Niños (1982–1983 and 1997–1998), where extensive damage was observed in the form of landslides and huge sediment loads.

In a final step, we compare the new data with published sediment flux data from across the Andes to identify relationships between the SSY and runoff. The results from this comparison reveal that watersheds in the Andean chain changed significantly in terms of size and location and there are no trend patterns shown.

In perspective, the aim of our study was to draw attention, at the continental scale, to the Peruvian coast as key areas for future research because of the highest complex spatio-temporal configuration.

Acknowledgements. This work was initiated as part of a Ph.D. dissertation at the La Molina Agrarian National University; it is financially supported by a doctoral research scholarship from the CONCYTEC (www.concytec.gob.pe) in cooperation with the FYNCYT. The authors are grateful to the funding through GREAT ICE team and the HYBAM observatory (www.ore-hybam.org) a join French–Peruvian program, associating the French Institut de Recherche pour le Développement (IRD, www.ird.fr), the SENAMHI (www.senamhi.gob.pe) and the UNALM (www.lamolina.edu.pe). We also give special thanks to the CHAVIMOCHIC project, which kindly provided the river discharge and SSC data. We also thank to Julien Nemery for valuable support and fruitful discussion.

References

Aalto, R., Dunne, T., and Guyot, J. L.: Geomorphic controls on Andean denudation rates, J. Geol., 114, 85–99, doi:10.1086/498101, 2006.

Aceituno, P.: On the functioning of the Southern Oscillation in the South American Sector, Part I: Surface climate, Mon. Weather Rev., 116, 505–524, doi:10.1175/1520-0493(1988)116<0505:OTFOTS>2.0.CO;2, 1988.

Adams, J. B., Sabol, D. E., Kapos, V., Filho, R. A., Roberts, D. A., and Smith, M. O.: Classification of multispectral images based on fractions of endmembers: application to land-cover change in the Brazilian Amazon, Remote Sens. Environ., 52, 137–154, 1995.

Agramonte, J. and Diaz, A.: Inventario preliminar del carbon mineral en el Peru, Instituto Geologico Minero y Metalurgico, Lima, Peru, p. 77, 1983.

Ahnert, F.: Functional relationships between denudation, relief and uplift in large, mid-latitude drainage basins, Am. J. Sci., 268, 243–263, 1970.

Andermann, C., Bonnet, S., and Gloaguen, R.: Evaluation of precipitation data sets along the Himalayan front, Geochem. Geophy. Geosy., 12, Q07023, doi:10.1029/2011GC003513, 2011.

Armijos, E., Crave, A., Vauchel, P., Fraizy, P., Santini, W., Moquet, J., Arevalo, N., Carranza, J., and Guyot, J. L.: Suspended sediment dynamics in the Amazon River of Peru, J. S. Am. Earth Sci., in press, 2013.

Baraer, M., McKenzie, J. M., Mark, B. G., Bury, J., and Knox, S.: Characterizing contributions of glacier melt and groundwater during the dry season in a poorly gauged catchment of the Cordillera Blanca (Peru), Adv. Geosci., 22, 41–49, doi:10.5194/adgeo-22-41-2009, 2009.

BCRP: Economic Synthesis for Ancash, Central Bank of Peru, Lima, Peru, 2009.

Betancourt, O., Narváez, A., and Roulet, M.: Small-scale gold mining in the Puyango River Basin, Southern Ecuador: a study of environmental impacts and human exposures, EcoHealth, 2, 1–10, 2005.

Bonnet, S. and Crave, A.: Landscape response to climate change: Insights from experimental modeling and implications for tectonic versus climatic uplift of topography, Geology, 32, 123–126, doi:10.1130/0091-7613(2003)031<0123:LRTCCI>2.0.CO;2, 2003.

Bookhagen, B. and Strecker, M. R.: Orographic barriers, high-resolution TRMM rainfall, and relief variations along the eastern Andes, Geophys. Res. Lett., 35, L06403, doi:10.1029/2007GL032011, 2008.

Bookhagen, B., Thiede, R. C., and Strecker, M. R.: Abnormal monsoon years and their control on erosion and sediment flux in the high, arid northwest Himalaya, Earth Planet. Sc. Lett., 231, 131–146, doi:10.1016/j.epsl.2004.11.014, 2005.

Bryan, L.: Gully-scale implications of rill network and confluence processes, in: Gully Erosion Under Global Change, edited by: Li, Y., Poesen, J., and Valentin, C., Sichuan Science and Technology, Chengdu, China, 73–95, 2004.

Carrascal-Miranda, E. and Suárez-Ruiz, I.: Short description of the Peruvian coal basins, Int. J. Coal Geol., 58, 107–117, doi:10.1016/j.coal.2003.05.004, 2004.

Carretier, S., Regard, V., Vassallo, R., Aguilar, G., Martinod, J., Riquelme, R., Pepin, E., Charrier, R., Herail, G., Farias, M., Guyot, J.-L., Vargas, G., and Lagane, C.: Slope and climate variability control of erosion in the Andes of Central Chile, Geology, G33735, doi:10.1130/G33735.1, in press, 2012.

Cerdan, O., Govers, G., Le Bissonnais, Y., Van Oost, K., Poesen, J., Saby, N., Gobin, A., Vacca, A., Quinton, J., Auerswald, K., Klik, A., Kwaad, F. J. P. M., Raclot, D., Ionita, I., Rejman, J., Rousseva, S., Muxart, T., Roxo, M. J., and Dostal, T.: Rates and spatial variations of soil erosion in Europe: a study based on erosion plot data, Geomorphology, 122, 167–177, doi:10.1016/j.geomorph.2010.06.011, 2010.

Condom, T., Escobar, M., Purkey, D., Pouget, J. C., Suarez, W., Ramos, C., Apaestegui, J., Tacsi, A., and Gomez, J.: Simulating the implications of glaciers' retreat for water management: a case study in the Rio Santa basin, Peru, Water Int., 37, 442–459, doi:10.1080/02508060.2012.706773, 2012.

Dadson, S. J., Hovius, N., Chen, H., Dade, W. B., Hsieh, M. L., Willett, S. D., Hu, J. C., Horng, M. J., Chen, M. C., Stark, C. P., Lague, D., and Lin, J. C.: Links between erosion, runoff variability and seismicity in the Taiwan orogen, Nature, 426, 648–651, doi:10.1038/nature02150, 2003.

DePloey, J. and Savat, J.: Contribution a l'etude de l'erosion par le splash, Z. Geomorphol., 12, 174–193, 1968.

Duvert, C., Gratiot, N., Némery, J., Burgos, A., and Navratil, O.: Sub-daily variability of suspended sediment fluxes in small mountainous catchments – implications for community-based river monitoring, Hydrol. Earth Syst. Sci., 15, 703–713, doi:10.5194/hess-15-703-2011, 2011.

Fang Fang, N., Hua Shi, Z., Li, L., Lu Guo, Z., Jin Liu, Q., and Lei, A.: The effects of rainfall regimes and land use changes on runoff and soil loss in a small mountainous watershed, Catena, 99, 1–8, doi:10.1016/j.catena.2012.07.004, 2012.

cc BY

Farnsworth, K. L. and Milliman, J. D.: Effects of climatic and anthropogenic change on small mountainous rivers: the Salinas River example, Global Planet. Change, 39, 53–64, doi:10.1016/S0921-8181(03)00017-1, 2002.

Farnsworth, K. L. and Milliman, J. D.: Effects of climatic and anthropogenic change on small mountainous rivers: the Salinas River example, Global Planet. Change, 39, 53–64, doi:10.1016/S0921-8181(03)00017-1, 2003.

Ferguson, R. I.: River loads underestimated by rating curves, Water Resour. Res., 22, 74–76, 1986.

Garreaud, R.: Multiscale Analysis of the Summertime Precipitation over the Central Andes, Mon. Weather Rev., 127, 901–921, doi:10.1175/1520-0493(1999)127<0901:MAOTSP>2.0.CO;2, 1999.

Garreaud, R. and Aceituno, P.: Interannual rainfall variability over the South American Altiplano, J. Climate, 14, 2779–2789, 2001.

Garreaud, R. and Fuenzalida, H.: The influence of the Andes on cutoff lows: a modeling study, Mon. Weather Rev., 135, 1596–1613, doi:10.1175/MWR3350.1, 2007.

Garreaud, R. and Rutllant, J.: Análisis meteorológico del los aluviones de Antofagasta y Santiago de Chile en el periodo 1991–1993, Atmósfera, 9, 251–271, 1996.

Garreaud, R. D.: The Andes climate and weather, Adv. Geosci., 22, 3–11, doi:10.5194/adgeo-22-3-2009, 2009.

Georges, C.: The 20th-century glacier fluctuations in the Tropical Cordillera Blanca (Peru), Arct. Antarct. Alp. Res., 36, 100–107, 2004.

Georges, C.: Recent Glacier Fluctuations in the Tropical Cordillera Blanca and Aspects of the Climate Forcing, Doctor en Ciencias Naturales, University of Innsbruck, 169 pp., 2009.

Giovanni, M., Horton, B., Garzione, C., McNulty, B., and Grove, M.: Extensional basin evolution in the Cordillera Blanca, Peru: stratigraphic and isotopic records of detachment faulting and orogenic collapse in the Andean hinterland, Tectonics, 29, 1–21, doi:10.1029/2010TC002666, 2010.

Göttlicher, D., Obregón, A., Homeier, J., Rollenbeck, R., Nauss, T., and Bendix, J.: Land-cover classification in the Andes of southern Ecuador using Landsat ETM+ data as a basis for SVAT modelling, Int. J. Remote Sens., 30, 1867–1886, doi:10.1080/01431160802541531, 2009.

Guyot, J. L.: Hydrogéochimie des fleuves de l'Amazonie bolivienne, ORSTOM, Paris, France, 261 pp., 1993.

cc BY

Harden, C.: Human impacts on headwater fluvial systems in the northern and central Andes, Geomorphology, 79, 249–263, doi:10.1016/j.geomorph.2006.06.021, 2006.

Henderson, K. A., Thompson, L. G., and Lin, P. N.: Recording of El Niño in ice core δ^{18}O records from Nevado Huascarán, Peru, J. Geophys. Res., 104, 63–65, 1999.

Houben, P., Wunderlich, J., and Schrott, L.: Climate and long-term human impact on sediment fluxes in watershed systems, Geomorphology, 108, 1–7, doi:10.1016/j.geomorph.2008.08.018, 2009.

Hovius, N., Stark, C. P., Chu, H.-T., and Lin, J.-C.: Supply and removal of sediment in a landslide-dominated mountain belt: Central Range, Taiwan, Geology, 108, 73–89, 2000.

HYBAM: Fourth Scientific Meeting of the ORE HYBAM, Lima, Peru, 2011.

Kirchner, J., Finkel, R. C., Riebe, C., Granger, D., Clayton, J. L., King, J. G., and Megahan, W. F.: Mountain erosion over 10 yr, 10 k.y., and 10 m.y. time scales, Geology, 29, 591–594, doi:10.1130/0091-7613(2001)029<0591:MEOYKY>2.0.CO;2, 2001.

Kirkby, M. J.: Measurement and theory of soil creep, Geology, 75, 359–378, 1967.

Korup, O. and Clague, J. J.: Natural hazards, extreme events, and mountain topography, Quaternary Sci. Rev., 28, 977–990, doi:10.1016/j.quascirev.2009.02.021, 2009.

Lague, D., Davy, P., and Crave, A.: Estimating uplift rate and erodibility from the area–slope relationship: examples from Brittany (France) and numerical modelling, Phys. Chem. Earth Pt. A, 25, 543–548, doi:10.1016/S1464-1895(00)00083-1, 2000.

Lague, D., Hovius, N., and Davy, P.: Discharge, discharge variability, and the bedrock channel profile, J. Geophys. Res., 110, F04006, doi:10.1029/2004JF000259, 2005.

Lamb, S. and Davis, P.: Cenozoic climate change as a possible cause for the rise of the Andes, Nature, 425, 792–797, doi:10.1038/nature02049, 2003.

Laraque, A., Bernal, C., Bourrel, L., Darrozes, J., Christophoul, F., Armijos, E., Fraizy, P., Pombosa, R., and Guyot, J. L.: Sediment budget of the Napo River, Amazon basin, Ecuador and Peru, Hydrol. Process., 23, 3509–3524, doi:10.1002/hyp.7463, 2009.

Lavado, W., Ronchail, J., Labat, D., Espinoza, J. C., and Guyot, J. L.: A basin-scale analysis of rainfall and runoff in Peru (1969–2004): Pacific, Titicaca and Amazonas drainages, Hydrolog. Sci. J., 57, 1–18, doi:10.1080/02626667.2012.672985, 2012.

Lavé, J. and Avouac, J. P.: Fluvial incision and tectonic uplift across the Himalayas of central Nepal, J. Geophys. Res., 106, 26561–26591, doi:10.1029/2001JB000359, 2001.

CC BY

Lin, G. W., Chen, H., Hovious, N., Horng, M. J., Dadson, S., Meunier, P., and Lines, M.: Effects of earthquake and cyclone sequencing on landsliding and fluvial sediment transfer in a mountain catchment, Earth Surf. Process., 33, 1354–1373, doi:10.1002/esp.1716, 2008.

Love, D., Clark, A., and Glover, K.: The lithologic, stratigraphic, and structural setting of the giant Antamina copper-zinc skarn deposit, Ancash, Peru, Econ. Geol., 99, 887–916, doi:10.2113/gsecongeo.99.5.887, 2004.

Malamuda, B. D. and Turcotte, D. L.: The applicability of power-law frequency statistics to floods, J. Hydrol., 322, 168–180, doi:10.1016/j.jhydrol.2005.02.032, 2006.

Marengo, J. A., Tomasella, J., and Uvo, C. R.: Trends in streamflow and rainfall in tropical South America: Amazonia, eastern Brazil, and northwestern Peru, J. Geophys. Res., 103, 1775–1783, doi:10.1029/97JD02551, 1998.

Mark, B. and Seltzer, G.: Tropical glacier meltwater contribution to stream discharge: a case study in the Cordillera Blanca, Peru, J. Glaciol., 49, 271–281, 2003.

McKean, J. A., Dietrich, W. E., Finkel, R. C., Southon, J. R., and Caffee, M. W.: Quantification of soil production and downslope creep rates from cosmogenic ^{10}Be accumulations on a hillslope profile, Geology, 21, 343–346, 1993.

McMahon, G., Evia, J., Pasco-Font, A., and Sanchez, J.: An Environmental Study of Artisanal, Small, and Medium Mining in Bolivia, Chile, and Peru, World Bank, Washington, D.C., 429 pp., 1999.

McNulty, B. and Farber, D.: Active detachment faulting above the Peruvian flat slab, Geology, 30, 567–570, 2002.

Milliman, J. D. and Syvitski, J. P.: Geomorphic/tectonic control of sediment transport to the ocean: the importance of small mountainous rivers, J. Geol., 100, 525–544, 1992.

Molina, A., Govers, G., Vanacker, V., Poesen, J., Zeelmaekers, E., and Cisneros, F.: Runoff generation in a degraded Andean ecosystem: interaction of vegetation cover and land use, Catena, 71, 357–370, 2007.

Molina, A., Govers, G., Poesen, J., Van Hemelryck, H., De Bievre, B., and Vanacker, V.: Environmental factors controlling spatial variation in sediment yield in central america mountain area, Geomorphology, 98, 176–186, 2008.

Molina, A., Vanacker, V., Mora, D., and Govers, G.: Complex land cover change, water and sediment yield in a degraded Andean environment, Hydrology, 472–473, 25—35, doi:10.1016/j.jhydrol.2012.09.012, 2012.

CC BY

Molnar, P. and England, P.: Late Cenozoic uplift of mountain ranges and global climate change: chicken or egg?, Nature, 346, 29–34, doi:10.1038/346029a0, 1992.

Montgomery, D. R.: Soil erosion and agricultural sustainability, Stanford University, P. Natl. Acad. Sci. USA, 104, 13268–13272, 2007.

Montgomery, D. R., Balca, G., and Willett, S.: Climate, tectonics, and the morphology of the Andes, Geology, 7, 579–582, 2001.

Morera, S.: Dinámica de la producción de sedimentos en la cuenca del río Santa, Magíster Scientiae en Recursos Hídricos, Universidad Nacional Agraria La Molina, Lima, Perú, 98 pp., 2010.

Pépin, E., Carretier, S., Guyot, J. L., and Escobar, F.: Specific suspended sediment yields of the Andean rivers of Chile and their relationship to climate, slope and vegetation, Hydrolog. Sci. J., 57, 1190–1205, 2010.

Petersen, G.: Mining and Metallurgy in Ancient Peru, Reaching New Peaks in Geoscience, Denver, CO, USA, 2010.

Philander, S. G. H.: El Niño Southern Oscillation phenomena, Nature, 302, 295–301, doi:10.1038/302295a0, 1983.

Pinet, P. and Souriau, M.: Continental erosion and large-scale relief, Tectonics, 7, 563–582, 1988.

Racoviteanu, A., Manley, W., Arnaud, Y., and Williams, M.: Evaluating digital elevation models for glaciologic applications: an example from Nevado Coropuna, Peruvian Andes, Global Planet. Change, 59, 110–125, 2007.

Rao, B., Santo, C., and Franchito, S.: A diagnosis of rainfall over South America during the 1997/98 El Nino Event, Part I: Validation of NCEP NCAR reanalysis rainfall data, J. Climate, 15, 502–511, 2002.

Raymo, M. E. and Ruddiman, W. F.: Tectonic forcing of late Cenozoic climate, Nature, 359, 117–122, doi:10.1038/359117a0, 1992.

Restrepo, J. D.: Water discharge and sediment load from the western slopes of the Colombian Andes with focus on Río San Juan, J. Geol., 108, 17–33, 2000.

Restrepo, J. D. and Kjerfve, B.: Magdalena River: interannual variability (1975–1995) and revised water discharge and sediment load estimates, J. Hydrol., 235, 137–149, 2000.

Restrepo, J. D., Kjerfve, B., Hermelin, M., and Restrepo, J. C.: Factors controlling sediment yield in a major South American drainage basin: the Magdalena River, Colombia, J. Hydrol., 316, 213–232, 2006.

Riebe, C., Kirchner, J., Granger, D., and Finkel, R. C.: Minimal climatic control on erosion rates in the Sierra Nevada, California, Geology, 29, 447–450, doi:10.1130/0091-7613(2001)029<0447:MCCOER>2.0.CO;2, 2001.

Rodríguez, E., Morris, C., and Belz, E.: A global assessment of the SRTM performance, Photogramm. Eng. Rem. S., 72, 249–260, 2006.

Roering, J., Kirchner, J., and Dietrich, W. E.: Evidence for nonlinear, diffusive sediment transport on hillslopes and implications for landscape morphology, Water Resour. Res., 35, 853–870, 1999.

Ronchail, J. and Gallaire, R.: ENSO and rainfall along the Zongo valley (Bolivia) from the Altiplano to the Amazon Basin, Int. J. Climatol., 26, 1223–1236, doi:10.1002/joc.1296, 2006.

Safran, E. B., Bierman, P. R., Aalto, R., Dunne, T., Whipple, K. X., and Caffee, M.: Erosion rates driven by channel network incision in the Bolivian Andes, Earth Surf. Process., 30, 1007–1024, doi:10.1002/esp.1259, 2005.

Schwartz, D. P.: Paleoseismicity and neotectonics of the Cordillera Blanca fault zone, northern Peruvian Andes, J. Geophys. Res., 93, 4712–4730, 1988.

Singh, A., Delcroix, T., and Cravatte, S.: Contrasting the flavors of El Niño-Southern Oscillation using sea surface salinity observations, J. Geophys. Res., 116, C06016, doi:10.1029/2010JC006862, 2011.

Slaymaker, O.: Drivers of mountain landscape change during the twenty-first century, J. Soil. Sediment., 10, 597–610, doi:10.1007/s11368-010-0194-6, 2010.

Small, E., Anderson, R., and Hancock, G.: Estimates of the rate of regolith production using ^{10}Be and ^{26}Al from an Alpine hillslope, Geomorphology, 27, 131–150, 1999.

Smith, R. B.: The influence of mountains on the atmosphere, Adv. Geophys., 21, 87–230, 1979.

Soden, B.: The sensitivity of the tropical hydrological cycle to ENSO, J. Climate, 13, 538–549, 2000.

Syvitski, J. P. M. and Kettner, A.: Sediment flux and the Anthropocene, Philos. T. Roy. Soc. A, 369, 957–975, doi:10.1098/rsta.2010.0329, 2011.

Syvitski, J. P. M. and Milliman, J. D.: Geology, geography, and humans battle for dominance over the delivery of fluvial sediment to the coastal ocean, Geology, 115, 1–19, doi:10.1086/509246, 2007.

Syvitski, J. P. M., Peckham, S., Hilberman, R., and Mulder, T.: Predicting the terrestrial flux of sediment to the global ocean: a planetary perspective, Sediment. Geol., 162, 5–24, doi:10.1016/S0037-0738(03)00232-X, 2003.

Tao, C., Qiongfang, L., Meixiu, Y., Guobin, L., Lipeng, C., and Xie, W.: Investigation into the impacts of land-use change on sediment yield characteristics in the upper Huaihe River basin, China, Phys. Chem. Earth A/B/C, 53–54, 1–9, doi:10.1016/j.pce.2011.08.023, 2012.

Tarras-Wahlberg, N. H. and Lane, S. N.: Suspended sediment yield and metal contamination in a river catchment affected by El Niño events and goldmining activities: the Puyango River Basin, Southern Ecuador, Hydrol. Process., 17, 3101–3123, doi:10.1002/hyp.1297, 2003.

Turcotte, D. L. and Greene, L.: A scale-invariant approach to flood frequency analysis, Stoch. Hydrol. Hydraul., 7, 33–40, 1993.

United-Nations: The Water Resources of Latin America and the Caribbean-Planning, Hazards and Pollution, United Nations Economic Commission for Latin America and the Caribbean, Santiago, Chile, 1990,

Vanacker, V., Molina, A., Govers, G., Poesen, J., Dercon, G., and Deckers, S: River channel response to short-term human-induced change in connectivity in Andean ecosystems, Geomorphology, 72, 340–353, doi:10.1016/j.geomorph.2005.05.013, 2005.

Vanmaercke, M., Poesen, J., Verstraeten, G., Vente, J., and Ocakoglu, F.: Sediment yield in Europe: spatial patterns and scale dependency, Geomorphology, 130, 142–161, doi:10.1016/j.geomorph.2011.03.010, 2011.

Vargas, G., Rutllant, J., and Ortlieb, L.: ENSO climate teleconnections andmechanisms for Holocene debris flows along the hyperarid coast of Western South America (17–24′ S), Earth Planet. Sc. Lett., 249, 467–483, doi:10.1016/j.epsl.2006.07.022, 2006.

Vente, J., Verduyn, R., Verstraeten, G., Vanmaercke, M., and Poesen, J.: Factors controlling sediment yield at the catchment scale in NW Mediterranean geoecosystems, J. Soil. Sediment., 11, 690–707, doi:10.1007/s11368-011-0346-3, 2011.

Verstraeten, G. and Poesen, J.: Factors controlling sediment yield from small intensively cultivated catchments in a temperate humid climate, Geomorphology, 40, 123–144, 2001.

Vuille, M., Kaser, G., and Irmgard, J.: Glacier mass balance variability in the Cordillera Blanca, Peru and its relationship with climate and the large-scale circulation, Global Planet. Change, 62, 14–28, doi:10.1016/j.gloplacha.2007.11.003, 2008.

Walling, D. E.: Assessing the accuracy of suspended sediment rating curves for a small basin, Water Resour. Res., 13, 531–538, 1977.

Walling, D. E.: Human impact on land-ocean sediment transfer by the world's rivers, Geomorphology, 79, 192–216, doi:10.1016/j.geomorph.2006.06.019, 2006.

cc BY

Ward, P., Bales, R., Verstraeten, G., Renssen, H., and Vandenberghe, J.: The impact of land use and climate change on late Holocene and future suspended sediment yield of the Meuse catchment, Geomorphology, 103, 89–400, doi:10.1016/j.geomorph.2008.07.006, 2009.

Wilson, J., Reyes, L., and Garayar, J.: Geología de los cuadrangulos de Mollebamba, Tayabamba, Huaylas, Pomabamba, Carhuaz, y Huari, Boletín, Servicio de Geología y Minería, Peru, p. 16, 1967.

Wohl, E.: Human impacts to mountain streams, Geomorphology, 79, 217–248, doi:10.1016/j.geomorph.2006.06.020, 2006.

Young, K. and Lipton, J.: Adaptive governance and climate change in the tropical highlands of western South America, Climatic Change, 78, 63–102, doi:10.1007/s10584-006-9091-9, 2006.

Zapata, M., Arnaud, Y., and Gallaire, R.: Inventario de glaciares de la Cordillera Blanca, 13th IWRA World Water Congreso, Montpellier, France, 2008.

Zhang, X. and Wen, A.: Current changes of sediment yields in the upper Yangtze River and its two biggest tributaries, China, Global Planet. Change, 41, 221–227, doi:10.1016/j.gloplacha.2004.01.008, 2004.

Zhang, X., Wang, X., and Yan, P.: Re-evaluating the impacts of human activity and environmental change on desertification in the Minqin Oasis, China, Environ. Geol., 55, 705–715, 2008.

Table 1. Description and interpretation of sedimentary and lithology information.

N	Formation name-code	Period	Rock type	Description
1	Chicama **Js-chic**	Jurassic	Sedimentary	Lutites and sandstone with quartzite
2	Santa-Carhuaz **Ki-sc**	Cretaceous	Sedimentary	Sandstone – quartzite – silststone with coal. Silt 80–95 %, sand (feldspar and quartz) 0–20 %, bitumen and coal 0–5 %.
3	Chimú **Ki-chi**	Cretaceous	Sedimentary	Sandstone and quartzite with lutites and coal. Quartz > 90 %, feldspar ± 5 %, silica colloid ± 5 %.
4	Goyllarisquizga **Ki-g**	Cretaceous	Sedimentary	Lutites sandstone and quartzite. Silt 80–95 %, sand (feldespar and quartz) 0–20 %, bitumen and coal 0–5 %.
5	Calipuy **Kti-vca**.	Cretaceous	Igneous	Volcanic pyroclastic rocks; dacite, rhyolite. Plagioclase 70–80 %, hornblende 20–25 %, magnetite.
6	Yungay **Ts-yu**	Triassic	Igneous	Dacite with rock fragments – biotite with feldspar matrix.
7	Granodiorite-Tonalite **T-gt**	Triassic	Igneous	Granite, granodiorite, diorite, tonalite – plagioclase 42 %, orthoclase 12 %, biotite 9 %, hornblende 4 %, quartz 20 %.
8	Aluvial **Q-al** Fluvio-Glacial **Q-fg**	Quaternary	Sedimentary	Tills and fluvio glacial formations – heterogeneous and unconsolidated rocks

Table 2. Distribution of the El Niño and La Niña events based on the Oceanic Niño Index; Source: National Oceanic and Atmospheric Administration (NOAA; http://www.esrl.noaa.gov/psd/enso/mei/table.html).

El Niño			La Niña		
Weak	Mod	Strong	Weak	Mod	Strong
1951–52	1986–87	1957–58	1950–51	1954–55	1955–56
1963–64	1987–88	1965–66	1956–57	1964–65	1973–74
1968–69	1994–95	1972–73	1962–63	1970–71	1975–76
1969–70	2002–03	1982–83	1967–68	1998–99	1988–89
1976–77		1991–92	1971–72	1999–00	
1977–78		1997–98	1974–75	2007–08	
2004–05		2009–10	1984–85	2010–11	
2006–07			1995–96		
			2000–01		

Table 3. Overview of the average to the highest amount of sediment production coming from the Andes mountains; each monitoring location is shown in Fig. 1. Santa (32), Tablachaca (33) and Condorcerro (34) rivers are the dark shaded points.

Code	Catchment	Catchment area (km^2)	Annual mean discharge (m^3 s^1)	Sediment yield (t km^{-2} yr^{-1})	Ocean	Period	Country	Source
1	Magdalena-Calamar	257 440	7200	560	Atlantic	1975–2005	Colombia	Pépin (2007)
2	Pilcomayo-Villamontes	87 350	292	2010	Atlantic	1977–2005	Bolivia	Pépin (2007)
3	Coca	5330	480	919	Atlantic	2001–2005	Ecuador	Laraque et al. (2009)
4	Napo FDO	12 400	1200	516	Atlantic	2001–2005	Ecuador	Laraque et al. (2009)
5	Napo	100 520	1486	1577	Atlantic	2001–2005	Ecuador	Laraque et al. (2009)
6	Huallaga-Chazuta	68 720	3010	1037	Atlantic	2004–2010	Peru	Armijos et al. (2013)
7	Marañon-Borja	114 280	4890	1295	Atlantic	2004–2010	Ecu-Peru	Armijos et al. (2013)
8	Ucayali-Atalaya	190 810	6540	1955	Atlantic	2009–2010	Peru	Armijos et al. (2013)
9	Béni-Rurrenabaque	68 900	1960	2293	Atlantic	2003–2010	Bolivia	HYBAM (2011)
10	Grande-Abapo	62 000	230	2581	Atlantic	2003–2007	Bolivia	HYBAM (2011)
11	Negro	4604	136	1730	Caribbean	2004–2010	Colombia	Restrepo et al. (2006b)
12	Carare	4943	90	2200	Caribbean	1985–1998	Colombia	Restrepo et al. (2006b)
13	Saldaña	7009	320	1271	Caribbean	1974–1999	Colombia	Restrepo et al. (2006b)
14	Lebrija	3500	90	1258	Caribbean	1979–1998	Colombia	Restrepo et al. (2006b)
15	La Miel	2121	243	1253	Caribbean	1975–1999	Colombia	Restrepo et al. (2006b)
16	Coello	1580	40	1035	Caribbean	1983–1999	Colombia	Restrepo et al. (2006b)
17	Cauca	59 615	2373	823	Caribbean	1978–1999	Colombia	Restrepo et al. (2006b)
18	Paez	4078	185	782	Caribbean	1972–2000	Colombia	Restrepo et al. (2006b)
19	Cabrera	2446	71	755	Caribbean	1982–1998	Colombia	Restrepo et al. (2006b)
20	Cocorna	799	56	745	Caribbean	1978–1999	Colombia	Restrepo et al. (2006b)
21	Samana	1490	181	625	Caribbean	1983–1999	Colombia	Restrepo et al. (2006b)
22	Yaguara	1386	15	593	Caribbean	1983–1999	Colombia	Restrepo et al. (2006b)
23	Nus	320	17	582	Caribbean	1983–1995	Colombia	Restrepo et al. (2006b)
24	Ceibas	220	5	581	Caribbean	1983–1999	Colombia	Restrepo et al. (2006b)
25	Maipo	370	16	1782	Pacific	1985–2006	Chile	Pépin et al. (2010)
26	Aconcagua	135	48	1356	Pacific	1966–1989	Chile	Pépin et al. (2010)
27	Tado	1600	261	1570	Pacific	1986–1994	Colombia	Restrepo et al. (2004)
28	Pte Guascas	8900	225	1714	Pacific	1972–1993	Colombia	Restrepo et al. (2004)
29	San Juan	14 000	2600	1150	Pacific	1970–1996	Colombia	Restrepo et al. (2006a)
30	Patia	14 000	317	972	Pacific	1972–1993	Colombia	Restrepo et al. (2006a)
31	Chira	20 000	159	1000	Pacific	–	Peru	Restrepo et al. (2006a)
32	Santa	6815	105	779	Pacific	2002–2010	Peru	this study
33	Tablachaca	3132	28	2204	Pacific	2002–2010	Peru	this study
34	Condorcerro	10 000	133	1517	Pacific	2000–2010	Peru	this study

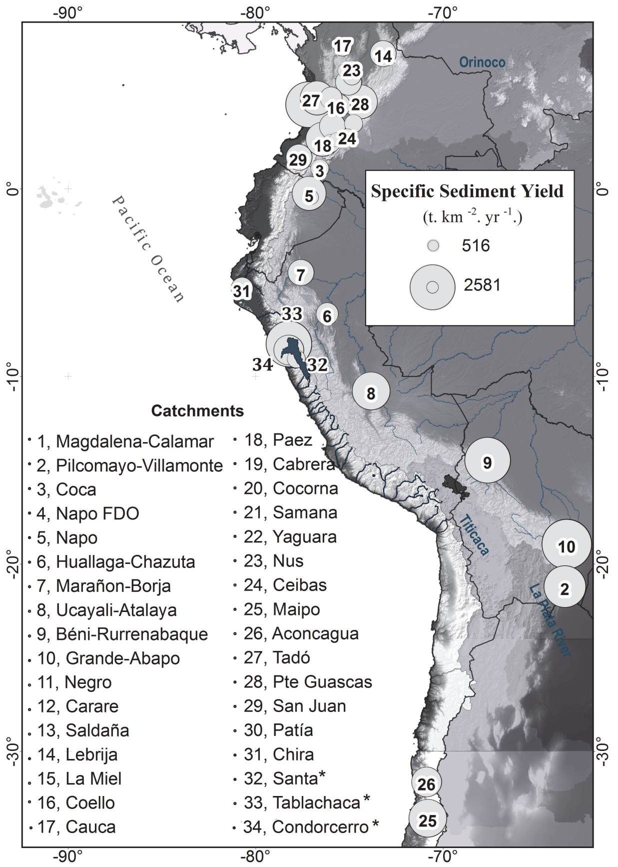

Fig. 1. Largest volumes of sediment delivered to the oceans, from the northern, central and southern Andean Cordillera. The size of the circles refers to the sediment yield rates. Numbers on the map and data sources correspond with Table 3. (*) study watersheds.

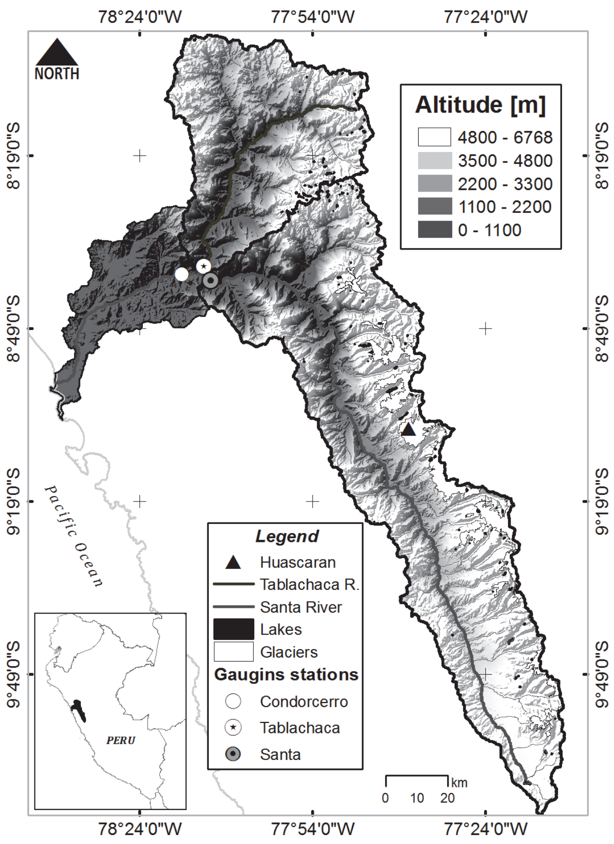

Fig. 2. Shaded-relief and elevation map of the Rio Santa watershed and Tablachaca sub-watershed in the central western part of the Andes (SRTM, 2002). Location of the monitoring stations.

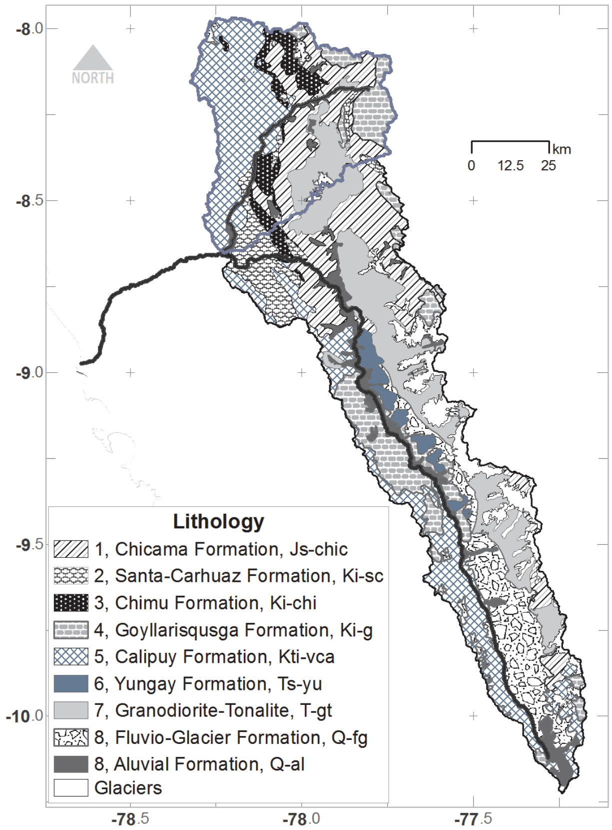

Fig. 3. Lithology distribution map of the Santa and Tablachaca catchments according to eight simplified formations. Units and descriptions in Table 1.

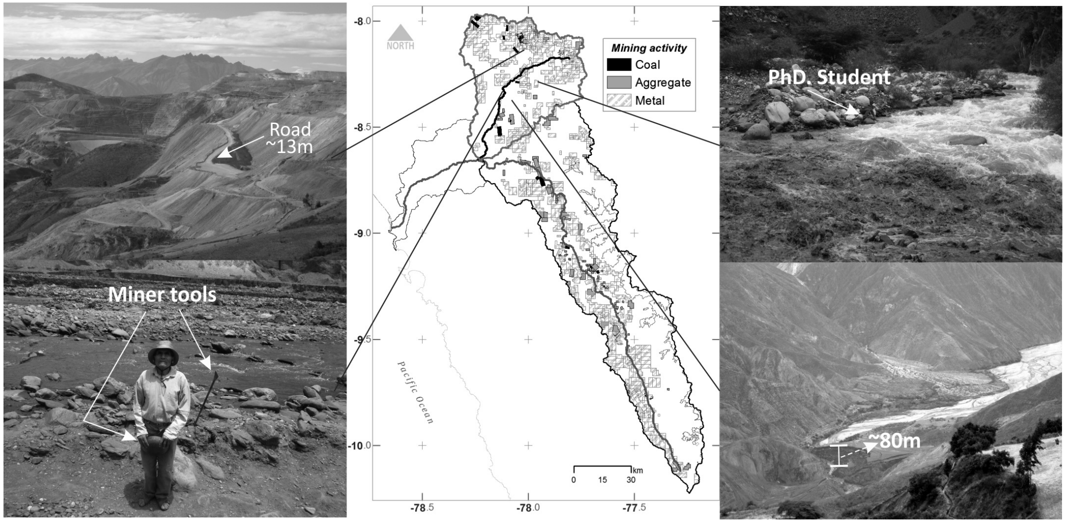

Fig. 4. The top view on the left shows the boom in large-scale mining in the upper basin. The bottom view on the left shows an informal miner using a gold panning technique during the dry season in the Tablachaca River. The centre view shows the distribution of mining concessions in the whole Santa Basin. The top view on the right shows the strong contrast between the higher SSC load carried out by Tablachaca River (left) and the lower SSC load in the Conchucos River (right) during the rainy season. The bottom view on the right shows a landslide from the Chimu formation; as a result, a natural dam was built in the riverbed many years ago.

Title Page
Abstract | Introduction
Conclusions | References
Tables | Figures
◀| |▶
◀ ▶
Back | Close
Full Screen / Esc
Printer-friendly Version
Interactive Discussion

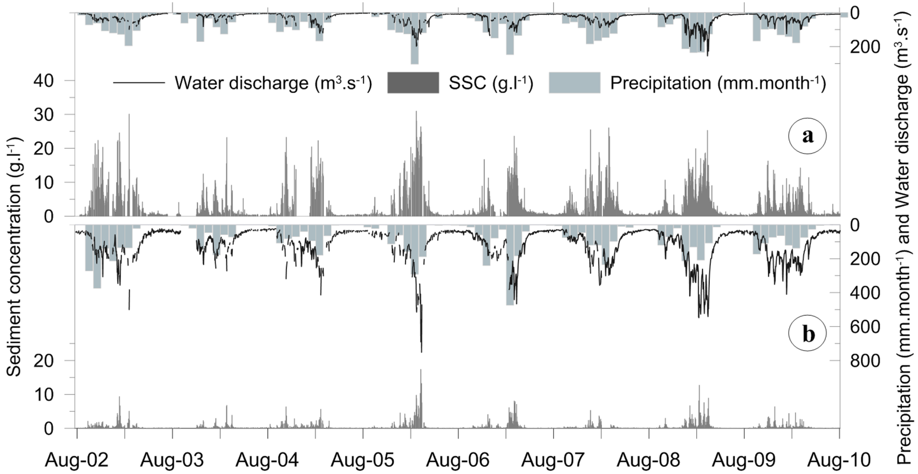

Fig. 5. Historic observed river discharge (on top), rainfall and sediment concentration. **(a)** Tablachaca mean annual: SSC 3.43 $\mathrm{g\,L^{-1}}$, discharge 28 $\mathrm{m^3\,s^{-1}}$ and rainfall 808.2 mm and **(b)** Santa stations mean annual: SSC 0.64 $\mathrm{g\,L^{-1}}$, 105.4 $\mathrm{m^3\,s^{-1}}$ and rainfall 810.4 mm.

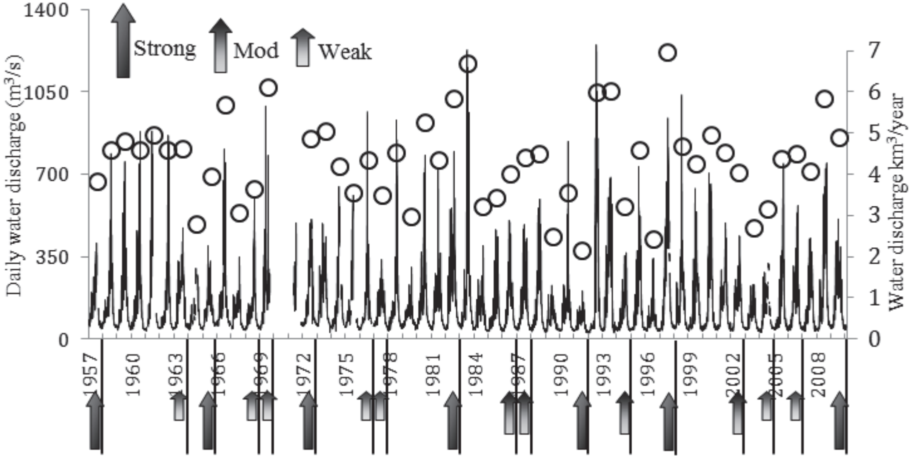

Fig. 6. Instantaneous historical outflow at the Condorcerro station ($m^3 s^{-1}$; 1957–2010), the average value is equal to $137 m^3 s^{-1}$ and S.D. 815.6. The arrow size indicates the Niño intensity, strong events (larger arrows), moderate events (medium-sized arrows) and weak events (small arrows); the dark thin bars show the end of the occurrence event. The circles show the annual mass balance of water discharge ($km^3 yr^{-1}$).

cc BY

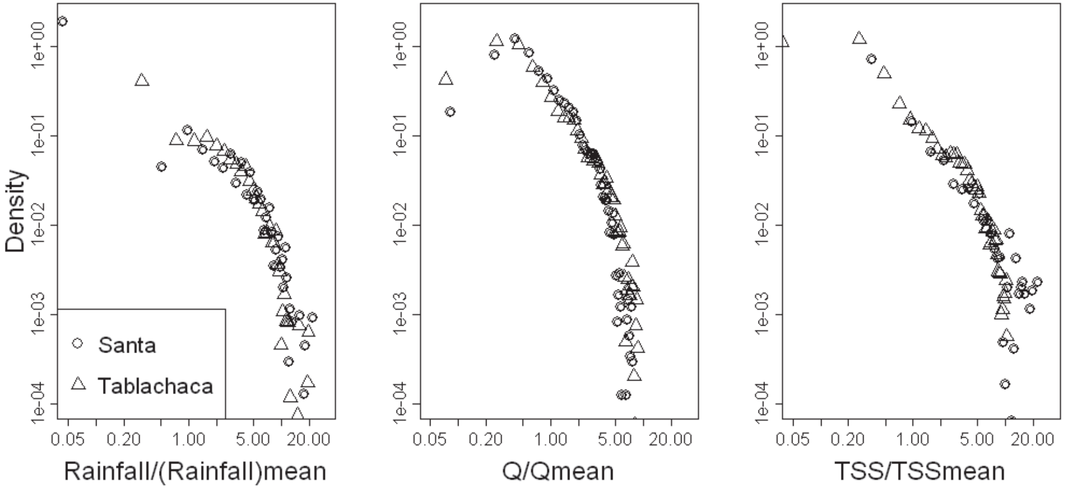

Fig. 7. Normalized probability density function based on precipitation **(a)**, water discharge **(b)** and suspended sediment concentration **(c)**.

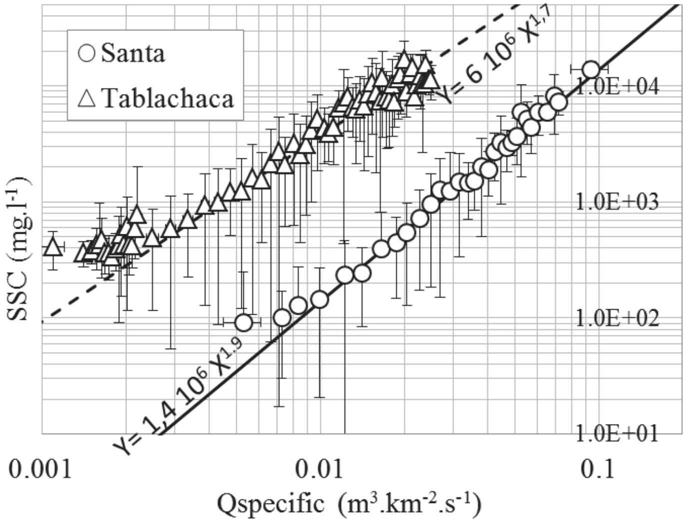

Fig. 8. Log-log relation of suspended sediment concentration (SSC, $\mathrm{mg\,L^{-1}}$) and corresponding specific sediment yield (SSY, $\mathrm{t\,km^{-2}\,yr^{-1}}$) at the Tablachaca and Santa stations, which makes a positive nonlinear relationship between the SSC and SSY. The dashed line is the power-law best fit for the all of the data collected in the Santa River. The dotted line is the power-law best fit for all of the data collected in the Tablachaca River. Bars represent the monthly variations.

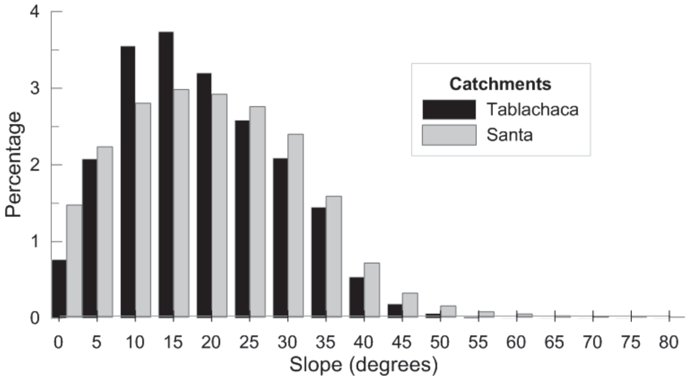

Fig. 9. Histogram showing the normalized percentage distribution of steep slopes generated from the SRTM for the upper Santa and Tablachaca catchment.

Title Page
Abstract | Introduction
Conclusions | References
Tables | Figures
◀| |▶
◀ ▶
Back | Close
Full Screen / Esc
Printer-friendly Version
Interactive Discussion

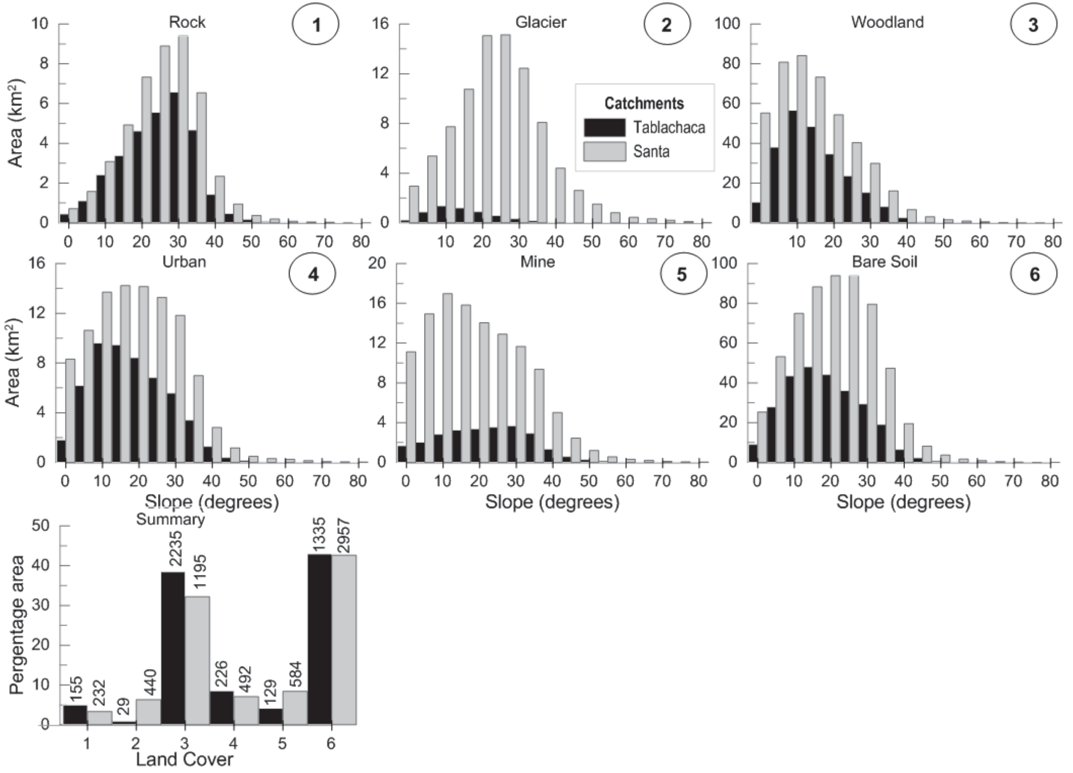

Fig. 10. Slope distribution as a function of land use in the Tablachaca and Santa catchments.

CC BY

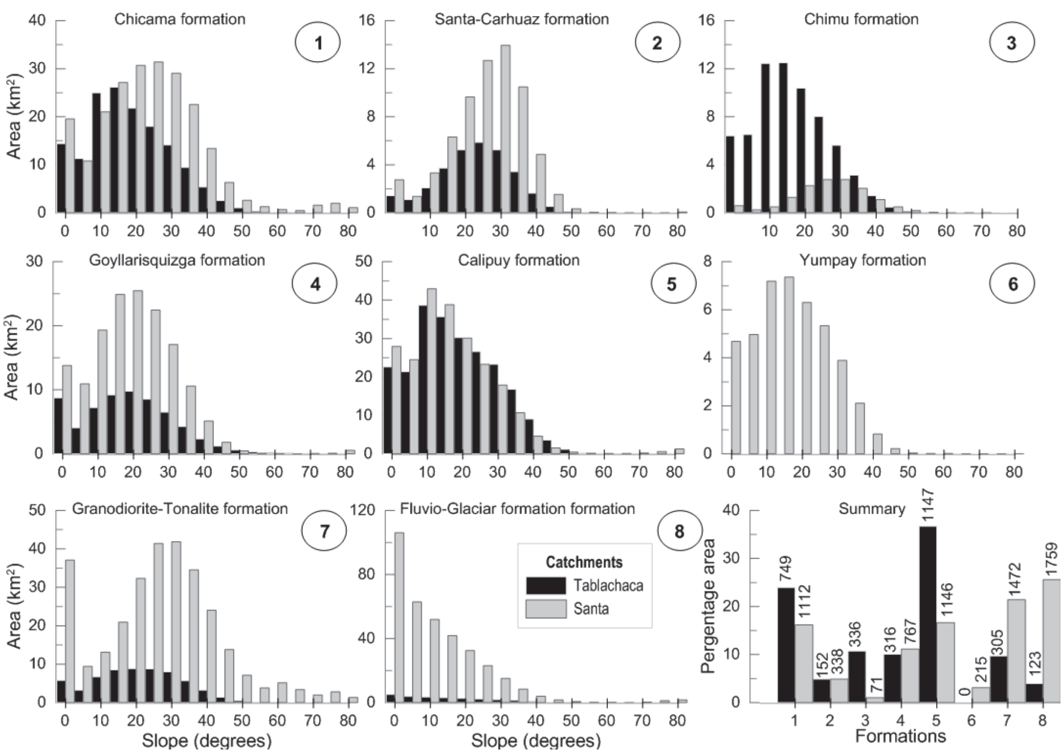

Fig. 11. Slope distribution as a function of the lithology in the Tablachaca and Santa catchments.

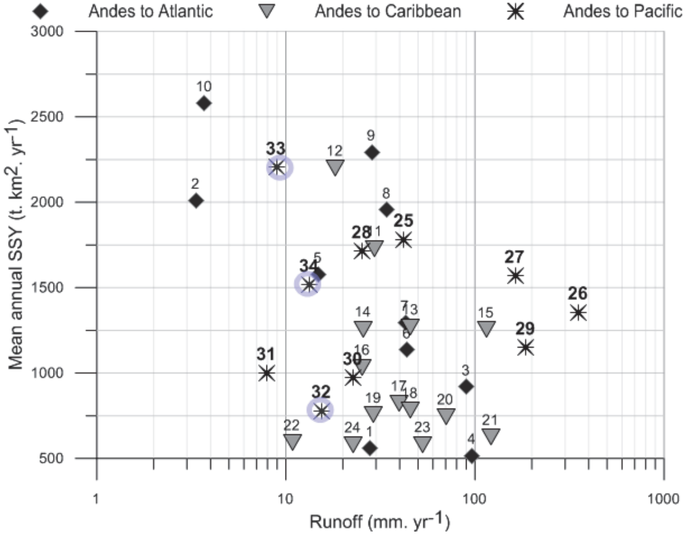

Fig. 12. Compilation of the SSY data from various sources (see Table 3). Comparison of the variation in the sediment yield with runoff for several mountainous rivers in the South American Andes. The Santa (32), Tablachaca (33) and Condorcerro (34) Rivers are the dark shaded points.

HESSD
10, 625–674, 2013

Title Page
Abstract Introduction
Conclusions References
Tables Figures
◀I ▶I
◀ ▶
Back Close
Full Screen / Esc
Printer-friendly Version
Interactive Discussion